Supplement of Nat. Hazards Earth Syst. Sci., 23, 2349–2363, 2023
https://doi.org/10.5194/nhess-23-2349-2023-supplement

Natural Hazards and Earth System Sciences
Open Access
EGU

Supplement of

Accounting for the effect of forest and fragmentation in probabilistic rock-fall hazard

Camilla Lanfranconi et al.

Correspondence to: Camilla Lanfranconi (c.lanfranconi2@campus.unimib.it)

Supplementary material

Table S1. Parameters of the tree-impact algorithm corresponding to a quercus robur tree forest: (i) height of stem [m], (ii) average height of trees [m], (iii) size of crown of tree [m], (iv) average DBH [m], (v) minimum distance between impacts [m], (vi) and maximum amount of kinetic energy that could be dissipated by a tree [J]

Parameter	**value**
height of stem	4.85
average height of trees [m]	14.97
size of crown of tree [m]	2.9
average diameter at breast height [m]	0.42
minimum distance between impacts [m]	10
maximum amount of kinetic energy that could be dissipated by a tree [kJ]	63.3

5

Table S2. Parameters of the fragmentation algorithm: (i) density of the generated fragments [kg/m^3], (ii) Young's elastic modulus of the rock [Pa], (iii) Poisson's coefficient of the rock [-], (iv) stress at break [Pa].

Parameter	**value**
Density of fragments [kg/m^3]	2700
Young's modulus [Pa]	4.0E+10
Poisson's ratio [-]	0.23
Limit stress [Pa]	2.2E+08

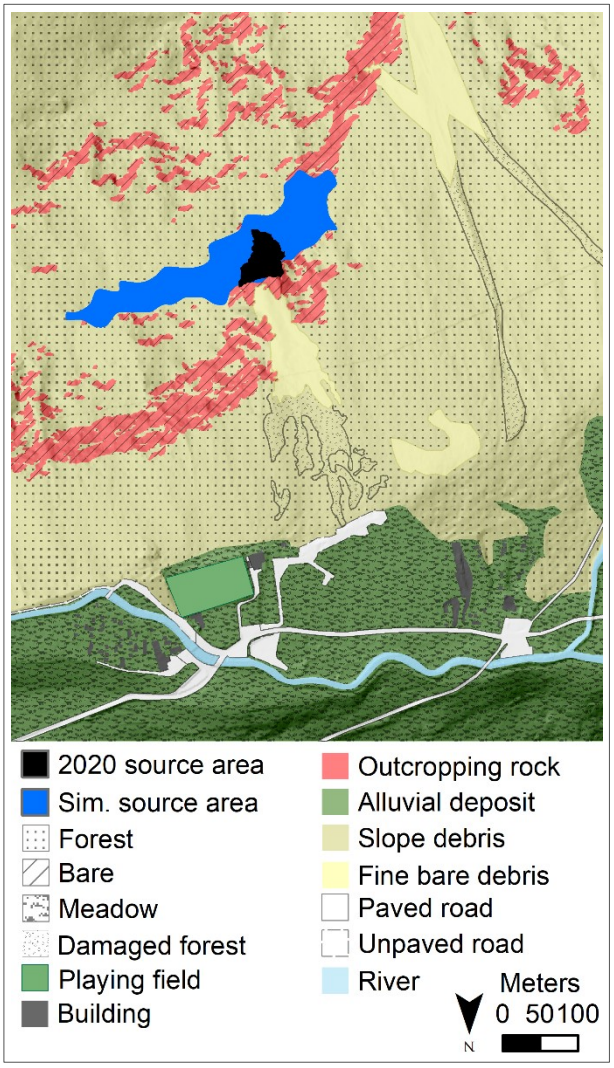

Figure S1 Unique conditions map for the Saint-Oyen case study. The associated values of normal (e_n) and tangential restitution (e_t) coefficients and of the friction coefficient (μ_s) are reported in Table 1.

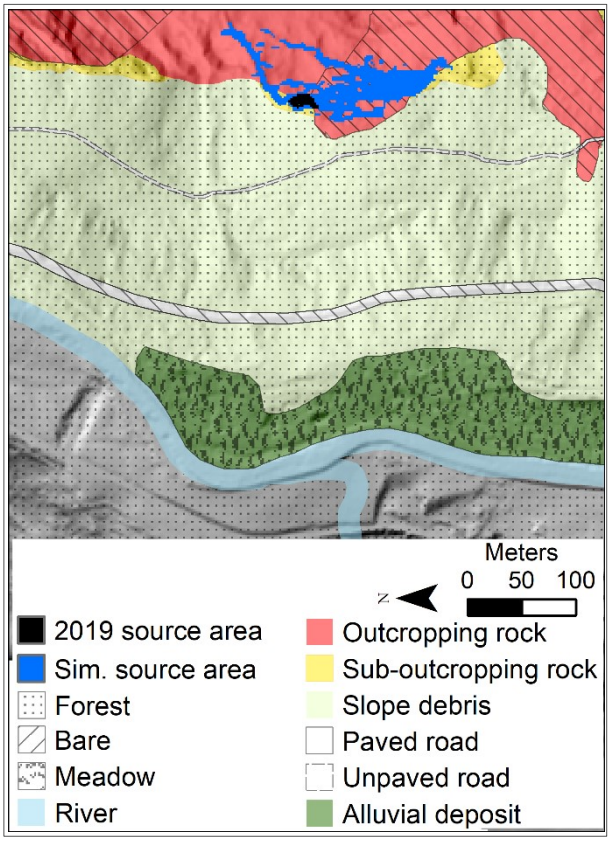

Figure S2 Unique conditions map for the Saint-Oyen case study. The associated values of normal (e_n) and tangential restitution (e_t) coefficients and of the friction coefficient (μ_s) are reported in Table 2.

10

Table S1 List of the numerical simulations together with source area information and the corresponding volumes.

ID	***Block volume***	***Launched blocks per cell***	***Number of source cells***	***Source Location***	***Specific algorithm activated***
SO_HS_Event	2020 event distribution	13	2,801	2020 event	N
SO_HS$_{tree}$_Event	2020 event distribution	13	2,801	2020 event	Y
SO_HS_S1	scenario S1	5	199	potential future source	N
SO_HS_S2	scenario S2	5	199	potential future source	N
SO_HS_S3	scenario S3	5	199	potential future source	N
SO_HS_S4	scenario S4	5	199	potential future source	N
SO_HS_S5	scenario S5	5	199	potential future source	N
SO_HS$_{tree}$_S1	scenario S1	5	199	potential future source	Y
SO_HS$_{tree}$_S2	scenario S2	5	199	potential future source	Y
SO_HS$_{tree}$_S3	scenario S3	5	199	potential future source	Y
SO_HS$_{tree}$_S4	scenario S4	5	199	potential future source	Y
SO_HS$_{tree}$_S5	scenario S5	5	199	potential future source	Y
R_HS_Event	2019 event distribution	100	46	2019 event	N
R_HS$_{frag}$_Event	2019 event distribution	100	46	2019 event	Y
R_HS$_{short}$_Event	2019 event distribution	100	46	2019 event	N
R_FI_S1	scenario S1	2	1,323	potential future source	N
RO_HS_S2	scenario S2	2	1,323	potential future source	N
RO_HS_S3	scenario S3	2	1,323	potential future source	N
RO_HS_S4	scenario S4	2	1,323	potential future source	N
RO_HS_S5	scenario S5	2	1,323	potential future source	N
RO_HS$_{frag}$ _S1	scenario S1	2	1,323	potential future source	Y
RO_HS$_{frag}$ _S2	scenario S2	2	1,323	potential future source	Y
RO_HS$_{frag}$ _S3	scenario S3	2	1,323	potential future source	Y
RO_HS$_{frag}$ _S4	scenario S4	2	1,323	potential future source	Y
RO_HS$_{frag}$ _S5	scenario S5	2	1,323	potential future source	Y

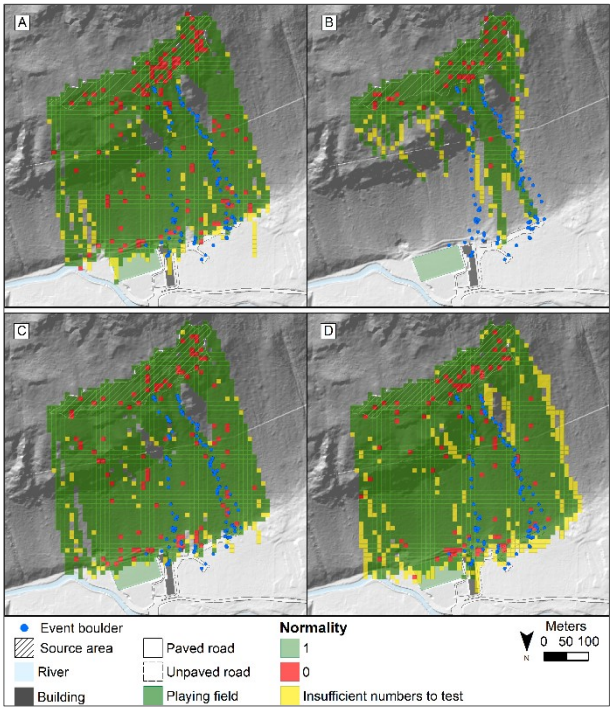

Figure S3 Normality results obtained from the Kolmogorov-Smirnov test in Saint-Oyen case study. Panel a) and b) refer to S1 scenario without and with adopting the tree-impact algorithm, respectively; panel c) and d) refer to S5 scenario without and with adopting the tree-impact algorithm, respectively

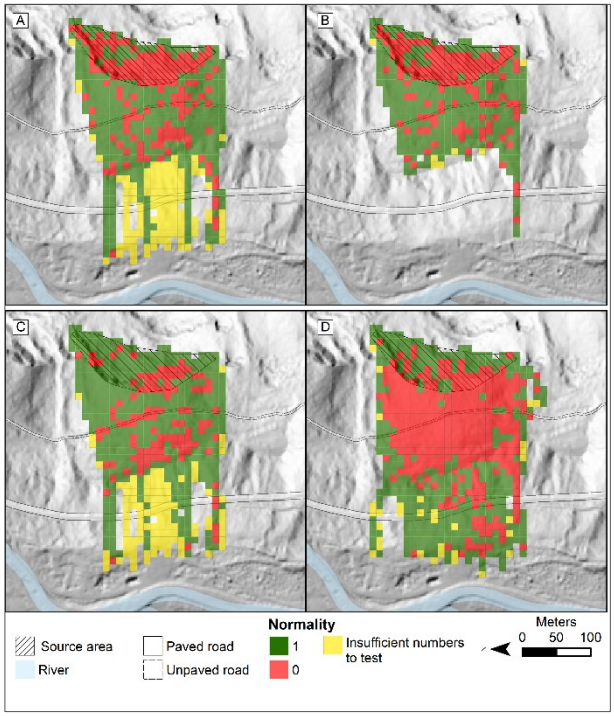

Figure S4 Normality results obtained from the Kolmogorov-Smirnov test in Roisan case study. Panel a) and b) refer to S1 scenario without and with adopting the fragmentation algorithm, respectively; panel c) and d) refer to S5 scenario without and with adopting the fragmentation algorithm, respectively.

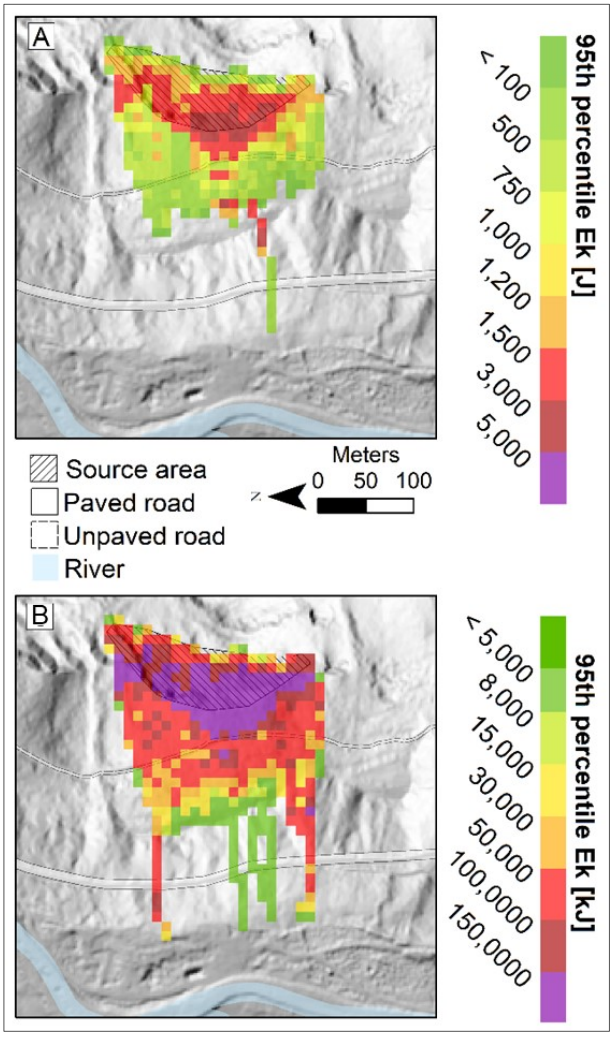

Figure S5 95th percentile values for the S1 (A) and S5 (B) scenarios with different HS_{short} model back-calibration approach. They differ from those obtained with the other calibration approach only in the models with implicit fragmentation: in A) only one trajectory passes the paved road and with lower energy than in the same case shown in ***Errore. L'origine riferimento non è stata trovata.****; also in B) far fewer trajectories pass the paved road unlike the same case in* ***Errore. L'origine riferimento non è stata trovata.****. In contrast, the scenarios modeled with the explicit fragmentation approach (Figure 4 B and D) do not differ significantly from their counterparts in because in both cases, when the fragmentation algorithm is*

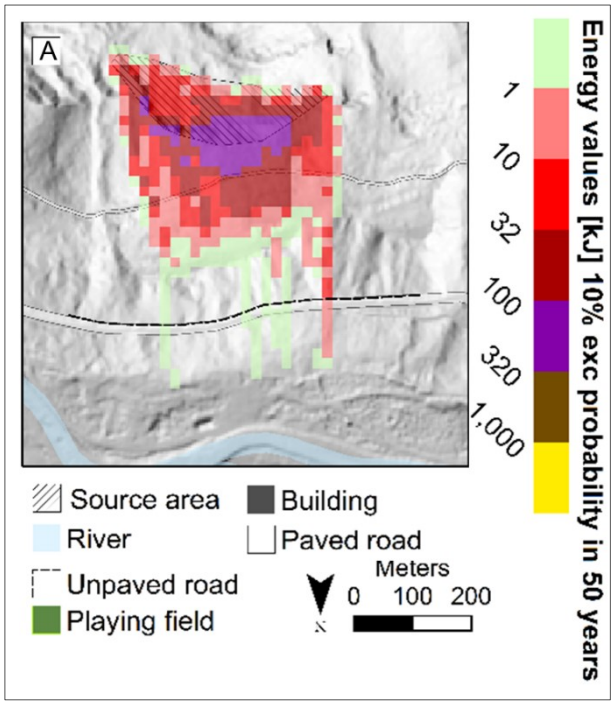

Figure S6 Hazard map for HS_{short} model. With respect to the HS model, the area involved is less sparse, crossing the paved road only in five spots. Only the rightmost corridor is characterized by an energy value associated to 10% exceedance probability in 50 years higher than 1 kJ.

activated, it is this that controls the block dynamics and thus the kinetic energies the most.

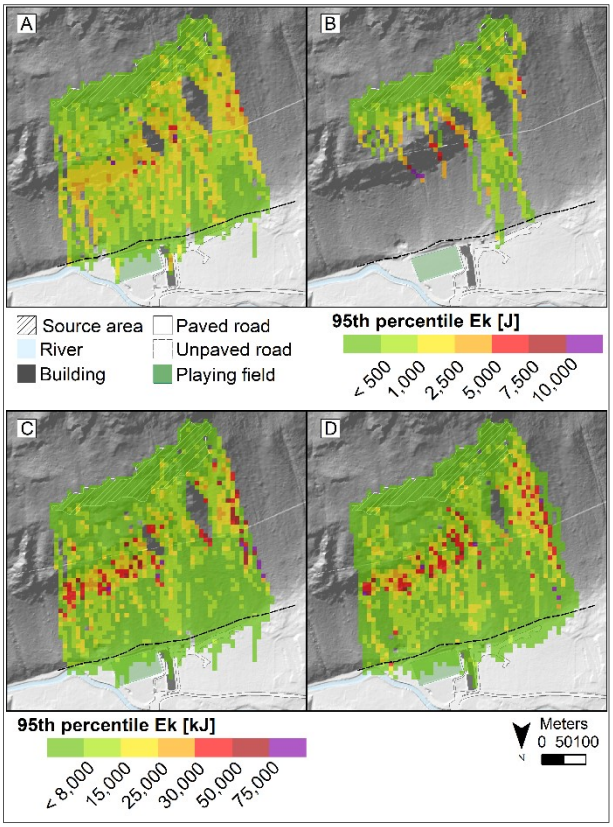

Figure S7 Distribution of kinetic energy of blocks along the slope in Saint-Oyen case study. The value of each cell corresponds to the 50th percentile of the kinetic energy of the blocks passing through that cell. Box A) scenario S1 (small blocks) HS, B) scenario S1 (small blocks) HS$_{frag}$, C) scenario S5 (large blocks) HS, D) scenario S5 (large blocks) HS$_{frag}$.

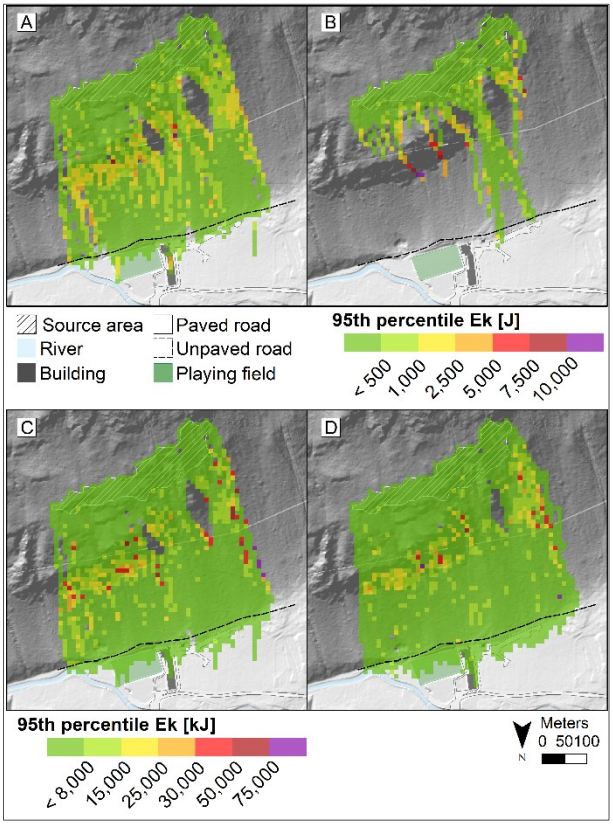

25 *Figure S8 Distribution of kinetic energy of blocks along the slope in Saint-Oyen case study. The value of each cell corresponds to the 25th percentile of the kinetic energy of the blocks passing through that cell. Box A) scenario S1 (small blocks) HS, B) scenario S1 (small blocks) HS$_{frag}$,*

C) scenario S5 (large blocks) HS, D) scenario S5 (large blocks) HS_{frag}.

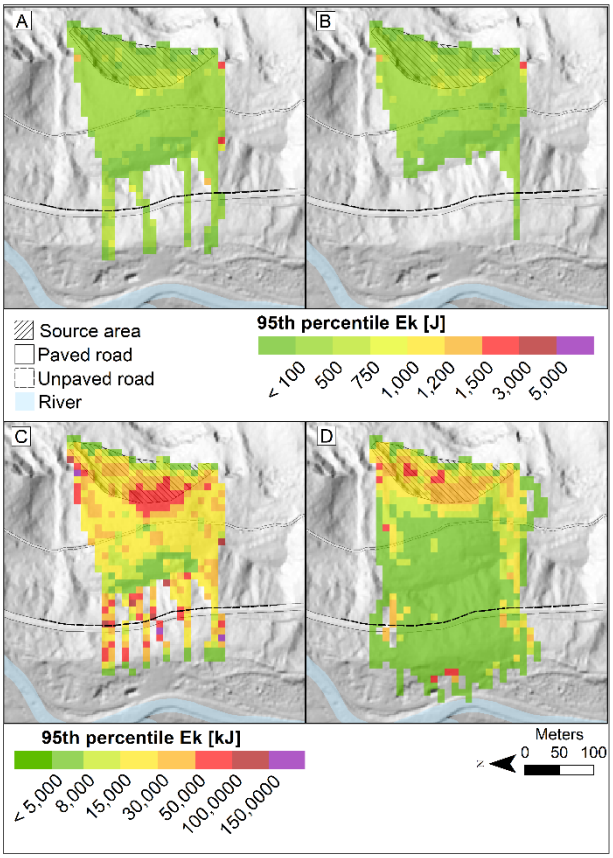

Figure S9 Distribution of kinetic energy of blocks along the slope in Roisan case study. The value of each cell corresponds to the 50th percentile of the kinetic energy of the blocks passing through that cell. Box A) scenario S1 (small blocks) HS, B) scenario S1 (small blocks) HS_{frag}, C) scenario S5 (large blocks) HS, D) scenario S5 (large blocks) HS_{frag}.

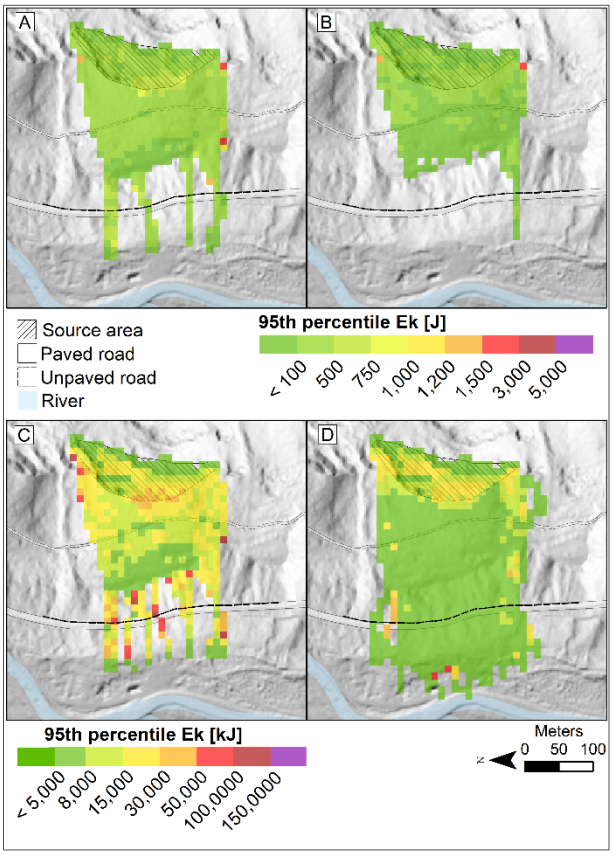

Figure S10 Distribution of kinetic energy of blocks along the slope in Roisan case study. The value of each cell corresponds to the 25th percentile of the kinetic energy of the blocks passing through that cell. Box A) scenario S1 (small blocks) HS, B) scenario S1 (small blocks) HS$_{frag}$, C) scenario S5 (large blocks) HS, D) scenario S5 (large blocks) HS$_{frag}$.

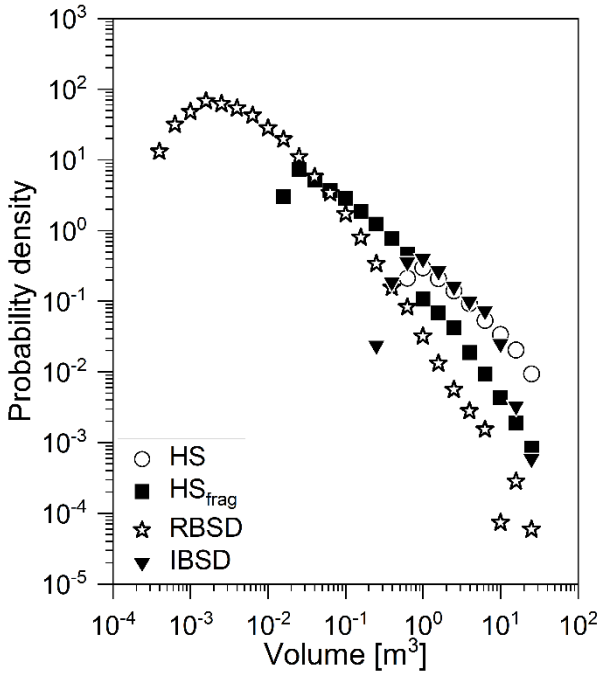

Figure S11 Comparison of the distributions of block size distributions surveyed in Roisan case study (IBSD and RBSD) and the simulated ones (HS and HSfrag)